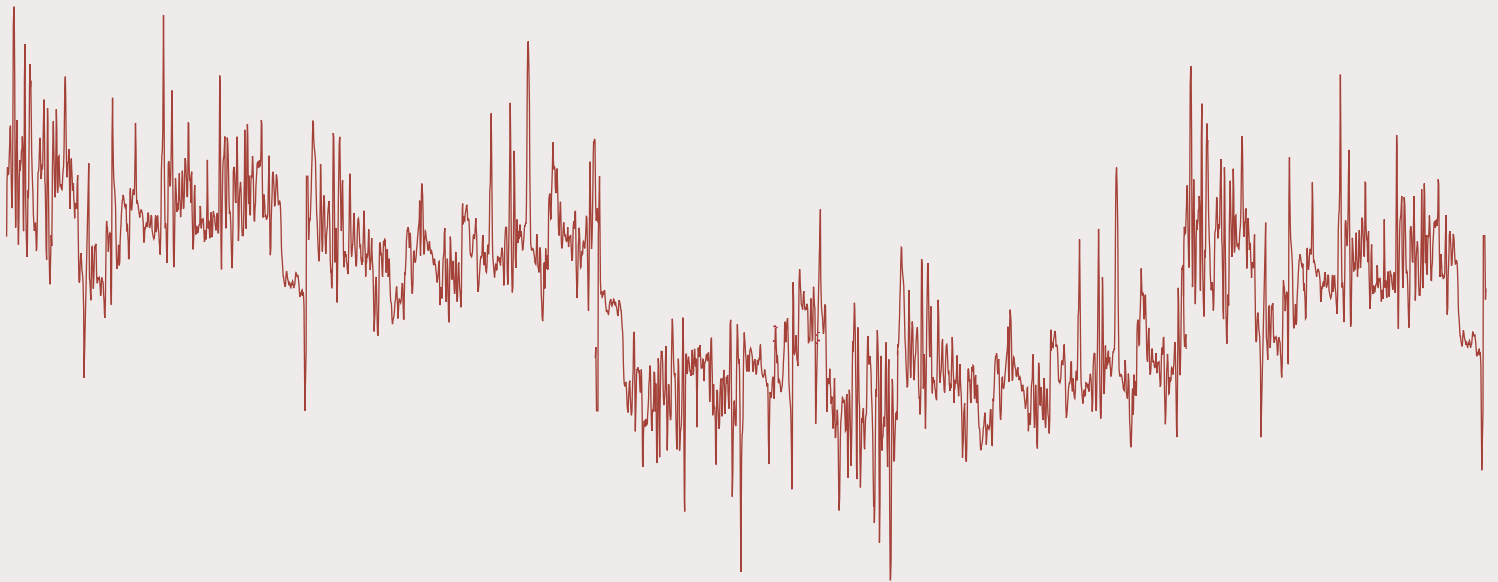


# Joint Inversion of Acoustic and Resistivity Data for the Estimation of Gas Hydrate Concentration



U.S. Geological Survey Bulletin 2190

# **Joint Inversion of Acoustic and Resistivity Data for the Estimation of Gas Hydrate Concentration**

*By* Myung W. Lee

U.S. Geological Survey Bulletin 2190

U.S. Department of the Interior  
U.S. Geological Survey

**U.S. Department of the Interior**  
Gale A. Norton, Secretary

**U.S. Geological Survey**  
Charles G. Groat, Director

This publication is only available online at:  
<http://geology.cr.usgs.gov/pub/bulletins/b2190/>

Version 1.0 2002

Any use of trade, product, or firm names in this publication  
is for descriptive purposes only and  
does not imply endorsement by the U.S. Government

Published in the Central Region, Denver, Colorado  
Manuscript approved for publication January 9, 2002  
Graphics by author and Gayle M. Dumonceaux  
Photocomposition by Gayle M. Dumonceaux  
Edited by L.M. Carter

# Contents

Abstract .....	1
Introduction .....	1
Acknowledgments .....	1
Theory .....	1
Inversion Equation .....	1
Derivatives for the Acoustics.....	2
Derivatives for the Resistivity .....	2
Modified Joint Inversion (MJI) .....	3
Inversion Examples .....	3
Original Joint Inversion (OJI) .....	3
Modified Joint Inversion Scheme (MJI) .....	4
Discussion .....	7
Weighted Error .....	7
Simultaneous Estimation of $c$ and $R_w$ .....	8
Behavior of the Joint Inversion Method .....	8
Understanding the Coupling Constant .....	8
Comparison of Various Inversion Results.....	9
Conclusion .....	10
References Cited .....	10

## Figures

1–7. Graphs showing:	
1. Result of original joint inversion of acoustics and resistivity .....	3
2. Estimated resistivity on connate water using original joint inversion and observed formation resistivity with respect to depth .....	5
3. Result of joint inversion of acoustics and resistivity using a constant resistivity of connate water $R_w=0.4$ ohm-meter .....	6
4. Result of modified joint inversion of acoustics and resistivity with a coupling constant $\gamma=1$ .....	6
5. Estimated resistivity of connate water using modified joint inversion with a coupling constant $\gamma=1$ and observed formation resistivity with respect to depth .....	7
6. Result of modified joint inversion of acoustics and resistivity with a coupling constant $\gamma=5$ .....	9
7. Result of averaging the individual gas hydrate estimates from $P$ -wave, $S$ -wave, and resistivity data .....	10

## Tables

1. Values used in the inversion .....	4
2. Modeled velocities and resistivity from the joint inversion .....	5
3. Results of estimated gas hydrate concentrations using various methods .....	5

# Joint Inversion of Acoustic and Resistivity Data for the Estimation of Gas Hydrate Concentration

By Myung W. Lee

## Abstract

Downhole log measurements, such as acoustic or electrical resistivity logs, are frequently used to estimate in situ gas hydrate concentrations in the pore space of sedimentary rocks. Usually the gas hydrate concentration is estimated separately based on each log measurement. However, measurements are related to each other through the gas hydrate concentration, so the gas hydrate concentrations can be estimated by jointly inverting available logs. Because the magnitude of slowness of acoustic and resistivity values differs by more than an order of magnitude, a least-squares method, weighted by the inverse of the observed values, is attempted. Estimating the resistivity of connate water and gas hydrate concentration simultaneously is problematic, because the resistivity of connate water is independent of acoustics. In order to overcome this problem, a coupling constant is introduced in the Jacobian matrix. In the use of different logs to estimate gas hydrate concentration, a joint inversion of different measurements is preferred to the averaging of each inversion result.

## Introduction

Gas hydrate has become an important research topic, because of its significance as a potential resource and because it is a controlling element in global warming, as well as a factor relevant to sea floor stability (Sloan and others, 1999). In this context, the estimation of in situ gas hydrate amounts present in sediments is important, and downhole well-log measurements are frequently used to quantify accumulations.

Gas hydrate in the pore space increases the elastic velocities and electrical resistivities of the host sediments. Therefore, downhole acoustic and electrical resistivity logs are most commonly used to identify and quantify natural gas hydrate resources.

Collett (1983, 1995) used downhole measurements extensively not only to identify the presence of gas hydrate in sediments and but also to quantify the amount of gas hydrate. Mathews (1986) used electrical resistivity logs to estimate gas hydrate saturation at the NW-Eileen #2 well, Alaska, and the deep sea drilling project Site 570 at Blake Ridge. Recently, Collett and Ladd (2000) also used resistivity logs to estimate gas hydrate amounts at Blake Ridge for Ocean Drill Program leg 164, Sites 994, 995, and 997, as did Miyairi and others (1999) at the Mallik 2L-38 gas hydrate research well, northeastern

Canada. Acoustic data have likewise been used to estimate hydrate concentrations. (For example, see Collett, 1983; 1995; Guerin and others, 1999; Lee and Collett, 1999; Lee, 2000.)

These estimates of gas hydrate were all derived based on measurements from only one log type, except that Miyairi and others (1999) used a statistical inversion of the logs. Because log measurements—*P*-wave, *S*-wave, and resistivity—are related to each other through the gas hydrate in the pore space, gas hydrate concentrations can be estimated by jointly inverting acoustic and resistivity logs.

This paper presents a method of estimating gas hydrate concentration by jointly inverting acoustic slowness (*P*-wave and *S*-wave slowness) and resistivity. Theoretical predictions of slownesses are computed from a weighted equation (Lee and others, 1996), and resistivities of sediments are computed from Archie's equation (1942). This inversion method was applied to the log data acquired at the Mallik 2L-38 gas hydrate research well, Mackenzie Delta, Canada (Dallimore and others, 1999).

## Acknowledgments

Well logs were acquired by Schlumberger Ltd. at the Mallik 2L-38 gas hydrate research well, which was drilled to investigate gas hydrate in a collaborative research project among Japan National Oil Company, Japan Petroleum Exploration Company, Geological Survey of Canada, and U.S. Geological Survey. I thank J.J. Miller and Y.K. Jin for many helpful comments.

## Theory

### Inversion Equation

Gas hydrate concentration can be estimated by a joint inversion of the acoustic (*P*- and *S*-wave) and resistivity data. Theoretical development of geophysical inversion methods has been extensive (Aki and Richards, 1980; Lines and Treitel, 1984; Tarantola, 1987). The derivation of the inversion method in this article closely follows Lee (1990). The method can be formulated by the Taylor series expansion of acoustic and resistivity equations, assuming that the unknown variables are the gas hydrate concentration (*c*) and the resistivity of the connate water ( $R_w$ ).

Column vectors  $O$  and  $T$  are defined as follows:

$O$  = column vector of the slownesses of  $P$ -wave ( $S_p$ ), and  $S$ -wave ( $S_s$ ), and the resistivity ( $R_t$ ).

$T$  = column vector of the computed or theoretical slowness of  $P$ -wave, slowness of  $S$ -wave, and resistivity.

Acoustics and resistivity can be approximated by the following equation:

$$T(m^{n+1}) = T(m^n) + \left(\frac{\partial T}{\partial c}\right)_n \Delta c + \left(\frac{\partial T}{\partial R_w}\right)_n \Delta R_w + \dots, \text{ or}$$

$$\begin{bmatrix} S_p(m^{n+1}) \\ S_s(m^{n+1}) \\ R_t(m^{n+1}) \end{bmatrix} = \begin{bmatrix} S_p(m^n) \\ S_s(m^n) \\ R_t(m^n) \end{bmatrix} + \begin{bmatrix} \partial S_p(m^n)/\partial c \\ \partial S_s(m^n)/\partial c \\ \partial R_t(m^n)/\partial c \end{bmatrix} \Delta c + \begin{bmatrix} 0 \\ 0 \\ \partial R_t(m^n)/\partial R_w \end{bmatrix} \Delta R_w \text{ or,}$$

$$\begin{bmatrix} S_p(m^{n+1}) \\ S_s(m^{n+1}) \\ R_t(m^{n+1}) \end{bmatrix} = \begin{bmatrix} S_p(m^n) \\ S_s(m^n) \\ R_t(m^n) \end{bmatrix} + \begin{bmatrix} \partial S_p(m^n)/\partial c & 0 \\ \partial S_s(m^n)/\partial c & 0 \\ \partial R_t(m^n)/\partial c & \partial R_t(m^n)/\partial R_w \end{bmatrix} \begin{bmatrix} \Delta c \\ \Delta R_w \end{bmatrix} \text{ or,}$$

$$T(m^{n+1}) = T(m^n) + G \Delta m \quad (1)$$

where  $m$  is a parameter vector consisting of  $c$  and  $R_w$ ,  $G$  is a  $3 \times 2$  Jacobian matrix,

$$\Delta c = c^{n+1} - c^n; \Delta R_w = R_w^{n+1} - R_w^n; \text{ and } \Delta m = m^{n+1} - m^n,$$

which is a column vector of  $(\Delta c, \Delta R_w)$ .

The least-squares solution of  $\Delta m$  in Equation (1) for a given observation  $O$  is attained by minimizing the mean-squared error ( $E$ ):  $E = (O - T)^2$ . Because the magnitude of resistivity is different from the values of slowness, a weighted least-squares method is attempted; the error function is defined as

$$E_i = ((O_i - T_i) / O_i)^2$$

where  $i = 1, 2$ , and  $3$ , which are values that represent indices for the  $P$ -wave slowness,  $S$ -wave slowness, and resistivity respectively;  $E_i$  is the component of the error function;  $T_i$  is the component of the computed value; and  $O_i$  is the component of the observed value. Then the solution can be written as

$$\Delta m = G_{we}^{-1} (I_3 - T_i / O_i) = G_{we}^{-1} E \quad (2)$$

where  $G_{we}^{-1}$  is the generalized inverse of the  $3 \times 2$  weighted Jacobian matrix (element of  $G_{we}$  is the element of  $G$  in Equation (1) divided by the corresponding observed value), and  $I_3$  is a  $3 \times 1$  column vector consisting of 1's. The generalized inverse of  $G_{we}^{-1}$  can be obtained using a singular value decomposition (SVD), and the solution can be written as

$$m^{n+1} = m^n + V \Lambda^{-1} U^T (I_3 - T_i / O_i) \quad (3)$$

where  $V$  is a  $2 \times 2$  matrix of orthonormal eigenvectors,  $U$  is a  $3 \times 3$  matrix of orthonormal eigenvectors,  $\Lambda$  is a diagonal matrix of two singular values, and the superscript  $T$  denotes a matrix transpose.

In this analysis, the derivatives for the Jacobian  $G$  are obtained from a weighted equation for the acoustic data (Lee and others, 1996) and the Archie equation (Archie, 1942) for the resistivity measurement.

## Derivatives for the Acoustics

A weighted equation (WE) can be written as follows, using slowness of the constituents (based on Lee and others, 1996):

$$S_p = W\phi(1-c)S_{p1} + [1 - W\phi(1-c)]S_{p2} \quad (4)$$

where

- $S_p$  = slowness by the WE
- $S_{p1}$  = slowness by the Wood equation
- $S_{p2}$  = slowness by the time average equation
- $W$  = a weighting factor
- $\phi$  = porosity
- $c$  = gas hydrate concentration.

The slowness by Wood equation ( $S_{p1}$ ) and slowness by time average equation ( $S_{p2}$ ) are given by

$$S_{p1} = \sqrt{\frac{\rho\phi(1-c)S_w^2}{\rho_w} + \frac{\rho\phi c S_h^2}{\rho_h} + \frac{\rho(1-\phi)S_m^2}{\rho_m}} \quad (5)$$

$$S_{p2} = \phi(1-c)S_w + \phi c S_h + (1-\phi)S_m$$

where  $\rho$ ,  $\rho_w$ ,  $\rho_h$ , and  $\rho_m$  are densities of gas-hydrate-bearing sediment, water, gas hydrate, and modified matrix, respectively;  $S_w$ ,  $S_h$ , and  $S_m$  are the slowness of water, gas hydrate, and modified matrix, respectively.

Shear-wave velocity is given by the following formula (Lee and others, 1996):

$$S_s = \frac{S_p}{\alpha(1-\phi) + \beta c} \quad (6)$$

where  $S_s$  is the slowness of the  $S$ -wave,  $\alpha$  and  $\beta$  are the ratios of  $S$ -wave velocity to  $P$ -wave velocity for the matrix of non-gas-hydrate-bearing sediments and for gas hydrate, respectively.

Using Equations (4), (5) and (6), the derivatives can be obtained as

$$\frac{\partial S_p}{\partial c} = -W\phi S_{p1} + W\phi S_{p2} + W\phi(1-c)\frac{\partial S_{p1}}{\partial c} + [1 - W\phi(1-c)]\frac{\partial S_{p2}}{\partial c} \quad (7)$$

where

$$\frac{\partial S_{p1}}{\partial c} = 0.5[-\rho\phi S_w^2/\rho_w + \rho\phi S_h^2/\rho_h]/S_{p1}, \text{ and}$$

$$\frac{\partial S_{p2}}{\partial c} = -\phi S_w + \phi S_h$$

$$\frac{\partial S_s}{\partial c} = \frac{(\partial S_p)/\partial c [\alpha(1-\phi) + c\beta\phi] - \beta\phi S_p}{[\alpha(1-\phi) + c\beta\phi]^2} \quad (8)$$

## Derivatives for the Resistivity

Water saturation ( $C_w$ ) from the Archie equation is given by

$$C_w = \left(\frac{aR_w}{\phi^m R_t^n}\right)^{1/n} \quad (9)$$

where  $a$ ,  $m$ , and  $n$  are constants,  $R_t$  is the resistivity of the formation,  $R_w$  is the resistivity of the connate water, and  $c$ ,

which is given by  $c = (1 - C_w)$ , is the gas hydrate concentration. Using Equation (9),

$$\begin{aligned} \frac{\partial R_t}{\partial c} &= \frac{nR_t}{1-c} \\ \frac{\partial R_t}{\partial R_w} &= \frac{R_t}{R_w} \end{aligned} \quad (10)$$

## Modified Joint Inversion (MJJ)

The solution in Equations (2) or (3) can be written in the following way using the element of Jacobian matrix ( $G_{ij}$ ).

$$\begin{aligned} c^{n+1} &= c^n + \frac{G_{11}E_1 + G_{21}E_2}{G_{11}^2 + G_{21}^2} \\ R_w^{n+1} &= R_w^n + \frac{-G_{31}G_{11}E_1 - G_{31}G_{21}E_2 + (G_{11}^2 + G_{21}^2)E_3}{G_{32}(G_{11}^2 + G_{21}^2)} \end{aligned} \quad (11)$$

The solution based on Equation (11) indicates that the resistivity measurement does not contribute directly to the estimation of gas hydrate concentration using the inversion scheme shown in Equation (1); there is no  $E_3$  component in the estimation of  $c$ . The only contribution of resistivity measurement to the joint inversion is through  $R_w$ , not through  $c$ ; accordingly, the estimated  $c$  from the  $P$ - and  $S$ -wave data is affected indirectly from the computed resistivity value, which provides minimum total error. In other words, the preceding joint inversion scheme computes the gas hydrate concentration using  $P$ -wave and  $S$ -wave data and attempts to fit the observed resistivity as closely as possible by changing  $R_w$ .

The reason for decoupling resistivity in Equation (11) for the estimation of  $c$  comes from the fact that the element of  $G_{12}$  and  $G_{22}$ , which are elements of the Jacobian matrix  $G$  shown in Equation (1), are zeros. In order to avoid this unwanted behavior, the elements of  $G_{12}$  and  $G_{22}$  are modified by adding an arbitrary constant ( $\gamma$ ). As can be seen from the numerical example given later, the magnitude of the constants controls the coupling between acoustics and resistivity in the joint inversion. The joint inversion with  $G_{12}=\gamma$  and  $G_{22}=\gamma$ , where  $\gamma$  is a non-zero constant, is called a modified joint inversion (MJJ), and  $\gamma$  is called a coupling constant in this report. The inversion scheme using the original formulation, shown in Equation (1), is called the original joint inversion (OJI) to differentiate from MJJ.

## Inversion Examples

### Original Joint Inversion (OJI)

In an investigation of the performance of the joint inversion using more than one type of measurements, parameters shown in table 1 were used. The initial values for  $c$  and  $R_w$  for the inversion were 0 and 0.4 ohm-meters (ohm-m), and both  $c$  and  $R_w$  were simultaneously estimated. Figure 1 shows the result of the joint inversion using  $P$ -wave,  $S$ -wave, and resistivity (PSR inversion) from the original inversion scheme shown

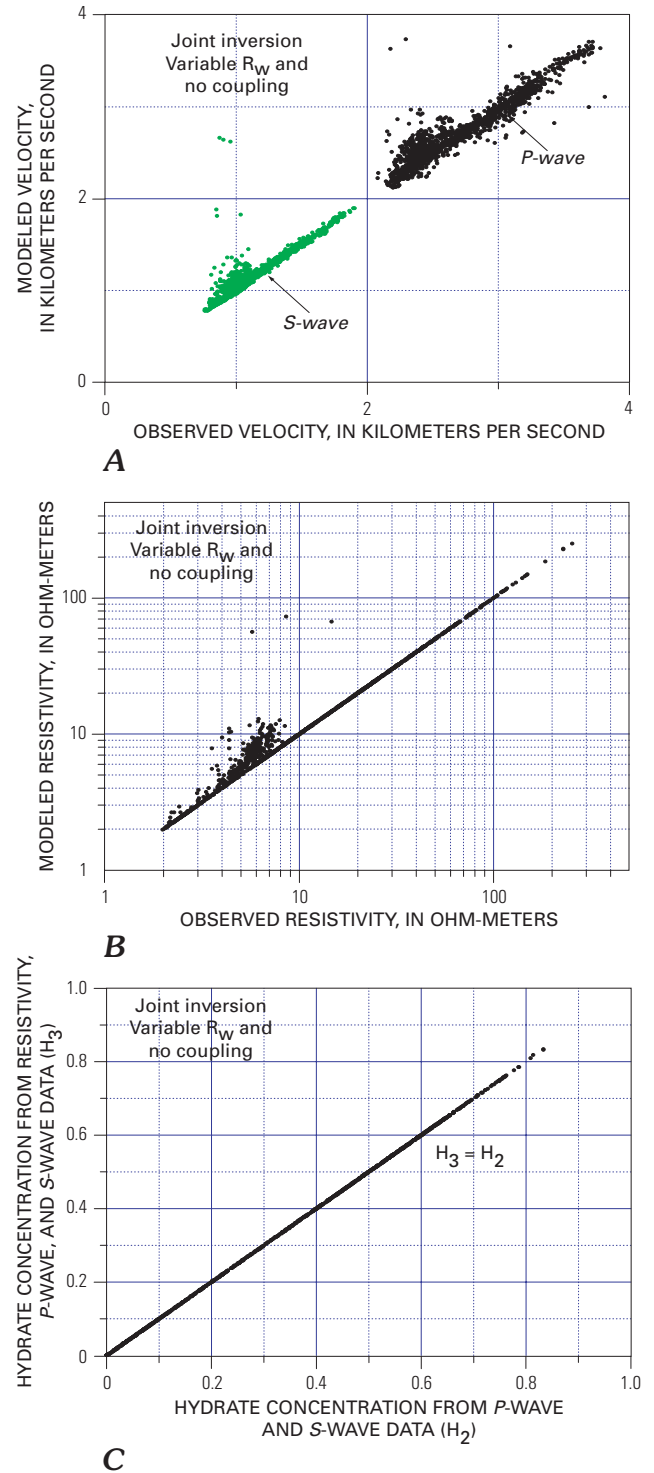


**Figure 1.** Graph showing the result of the original joint inversion of acoustics and resistivity. Both gas hydrate concentration ( $c$ ) and the resistivity of connate water ( $R_w$ ) were simultaneously estimated. *A*, Cross plot of modeled velocities versus observed velocities. *B*, Cross plot of modeled resistivity versus observed resistivity. *C*, Cross plot of gas hydrate concentration estimated from acoustics versus that estimated from the joint inversion of acoustics and resistivity.

in Equation (1). Figure 1A shows the comparison of the observed velocity versus the modeled (computed) velocity. Most of the scattering is about a 45° line and the average computed  $P$ -wave velocity is about 1 percent higher than the

**Table 1.** Values used in the inversion.

Meaning	Symbol	Value	Remarks
Slowness of hydrate (s/m)	$S_h$	0.303	Type 1 gas hydrate
Slowness of water (s/m)	$S_w$	0.667	
Slowness of modified matrix (s/m)	$S_m$	0.203	30% volume clay content
Ratio of $V_s/V_p$	$\alpha$	0.56	Non-hydrate-bearing sediment
Ratio of $V_s/V_p$	$\beta$	0.51	Type 1 gas hydrate
Density of gas hydrate (g/cm <sup>3</sup> )	$\rho_h$	0.91	Type 1 gas hydrate
Density of water (g/cm <sup>3</sup> )	$\rho_w$	1.0	
Density of modified matrix (g/cm <sup>3</sup> )	$\rho_m$	2.65	
Weighting factor	$W$	1.44	
Cementation factor	$m$	1.95	Archie's Equation
Archie's parameter	$a$	1.05	Archie's Equation
Exponent	$n$	1.9386	Archie's Equation
Resistivity of water (ohm-m)	$R_w$	0.4	

observed velocity; the average computed  $S$ -wave velocity is 3 percent higher than the observed velocity (table 1). When only  $P$ -wave and  $S$ -wave velocities are used in the joint inversion (PS inversion), the modeled velocities are  $2.72 \pm 0.40$  kilometers per second (km/s) and  $1.21 \pm 0.27$  km/s for the  $P$ -wave and  $S$ -wave velocities, respectively. The modeled  $P$ -wave velocity from PS inversion more closely matches the observed velocity, but there is little difference in  $S$ -wave velocities.

Figure 1B shows the modeled and observed resistivity (from PSR inversion). Unlike the acoustic case, the computed resistivities are almost identical to those observed when  $R_t$  is greater than about 9 ohm-m. Modeled resistivities are higher than the observed resistivities when  $R_t$  is less than 9 ohm-m.

The comparison between estimated gas hydrate concentrations using only acoustic data and estimates based on combined acoustic and resistivity data is shown in figure 1C. As the theory predicts, the estimates are almost identical. As indicated in Equation (11), the gas hydrate concentration is estimated mostly from  $P$ - and  $S$ -wave data, and  $R_w$  is estimated by matching the observed  $R_t$  with the theoretical prediction.

Figure 2, showing the estimated  $R_w$  for the preceding example and the observed resistivity ( $R_t$ ) with respect to depth, indicates that the majority of estimated  $R_w$  values falls between 0.2 ohm-m and 1 ohm-m. A cross plot between the  $R_w$  and the observed resistivity ( $R_t$ ) indicates that estimated  $R_w$  is roughly proportional to the observed resistivity. Figure 2 also indicates that the estimated  $R_w$  appears to decrease with respect to the increasing depth. A least-squares fitting curve for the estimated  $R_w$  is given by  $R_w = 2.72 - 0.00214D$ , where  $D$  is depth in meters (m). At  $D = 1,000$  m, the estimated  $R_w$  is 0.58 ohm-m. The accuracy of the estimated  $R_w$  is discussed later.

Figure 3 shows the PSR inversion result when  $R_w$  is assumed to be a constant of 0.4 ohm-m. When  $R_w$  is a constant,

Equation (11) cannot be used for the inversion solution, and only the gas hydrate concentration,  $c$ , is estimated. Therefore, the Jacobian matrix shown in Equation (1) is a  $3 \times 1$  column matrix. In this case, the solution is given by:

$$c^{n+1} = c^n + \frac{G_{11}E_1 + G_{21}E_2 + G_{31}E_3}{G_{11}^2 + G_{21}^2 + G_{31}^2} \quad (12)$$

If the original solution form is used, the results of the PSR inversion using a constant  $R_w$  approach the results of the resistivity inversion (R inversion) as shown later.

The modeled resistivity is similar to the observed resistivity when resistivity is greater than 8 ohm-m (fig. 3B), and modeled acoustics show a large scattering around a  $45^\circ$  line (fig. 3A). Table 2 indicates that the average of the modeled  $P$ -wave velocity is  $2.84 \pm 0.46$  km/s, which is about 4 percent higher compared to the observed value, and  $1.35 \pm 0.33$  km/s for the  $S$ -wave velocity, which is about 15 percent higher. The estimated gas hydrate concentrations using acoustic and resistivity data are much higher than those based on acoustic data only (PS inversion), as shown in figure 3C and table 3.

## Modified Joint Inversion Scheme (MJI)

Result of the MJI, estimating  $c$  and  $R_w$  simultaneously with  $\gamma=1$ , is shown in figure 4. Figure 4A shows the comparison of the observed velocity versus the modeled (computed) velocity. Like results shown in figure 1A, the scattering between the modeled and observed velocities is about the  $45^\circ$  line, and the average computed  $P$ -wave velocity is about 2 percent higher than the observed velocity; the average computed  $S$ -wave velocity is about 5 percent higher than the observed velocity (table 2).

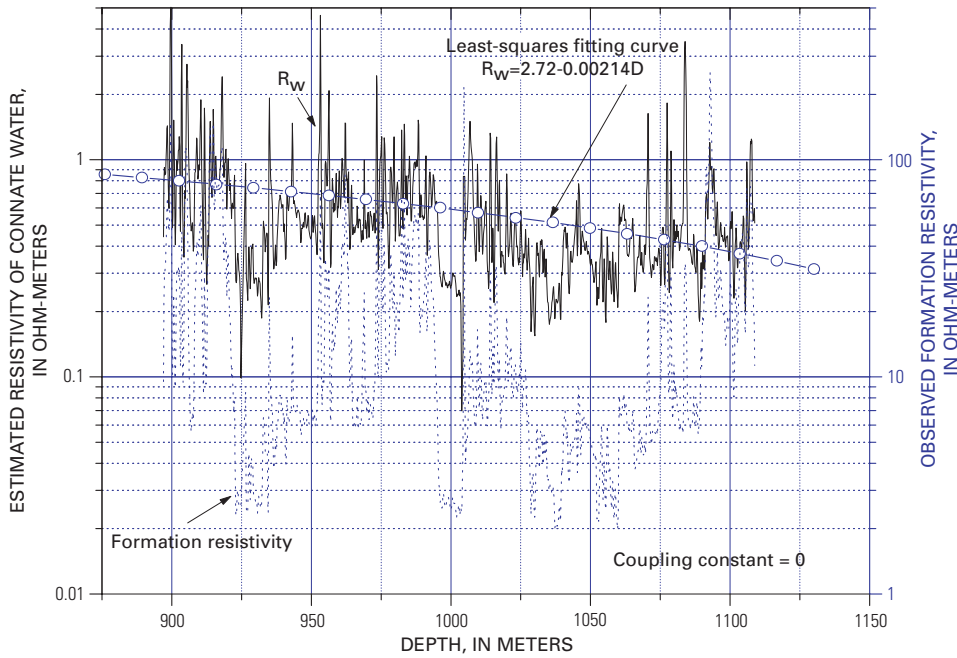


**Figure 2.** Graph showing estimated resistivity of connate water ( $R_w$ ) using original joint inversion and observed formation resistivity with respect to depth.  $D$ , depth in meters.

**Table 2.** Modeled velocities and resistivity from the joint inversion.

[Percentage (%) in parentheses is the fractional error between observed and modeled values. Model 1, result from the joint inversion estimating  $c$  and  $R_w$  simultaneously using the original equation; Model 2, result from joint inversion estimating  $c$  with a constant  $R_w = 0.4$  ohm-m; Model 3, result from the modified joint inversion with  $\gamma = 1$  and estimating  $c$  and  $R_w$  simultaneously]

	Observed	Model 1 (OJI)	Model 2 (Constant $R_w$ )	Model 3 (MJI)
$V_p$ (km/s)	$2.72 \pm 0.39$	$2.75 \pm 0.38$ (1%)	$2.84 \pm 0.46$ (4%)	$2.78 \pm 0.40$ (2%)
$V_s$ (km/s)	$1.17 \pm 0.26$	$1.21 \pm 0.27$ (3%)	$1.35 \pm 0.33$ (15%)	$1.23 \pm 0.28$ (5%)
$R_t$ (ohm-m)	$17.97 \pm 24.99$	$18.44 \pm 23.93$ (3%)	$17.99 \pm 23.32$ (0%)	$18.26 \pm 23.89$ (2%)

**Table 3.** Results of estimated gas hydrate concentrations using various methods.

Measurement	Estimation <sup>1</sup>	Estimation <sup>2</sup>	Remarks
P-wave	$0.29 \pm 0.25$	$0.39 \pm 0.23$	
S-wave	$0.28 \pm 0.24$	$0.36 \pm 0.21$	
Resistivity	$0.33 \pm 0.30$	$0.49 \pm 0.24$	Constant $R_w = 0.4$ ohm-m
P- and S-wave	$0.28 \pm 0.24$	$0.37 \pm 0.22$	Joint inversion
P-, S-wave, and resistivity	$0.28 \pm 0.24$	$0.37 \pm 0.22$	OJI with variable $R_w$
P-, S-wave, and resistivity	$0.30 \pm 0.26$	$0.39 \pm 0.23$	MJI with $\gamma=1$ and variable $R_w$
P-, S-wave, and resistivity	$0.32 \pm 0.30$	$0.47 \pm 0.24$	MJI with $\gamma=5$ and $R_w = 0.4$ ohm-m
P-, S-wave, and resistivity	$0.32 \pm 0.30$	$0.47 \pm 0.24$	OJI with $R_w = 0.4$ ohm-m
P- and S- wave	$0.28 \pm 0.25$	$0.36 \pm 0.22$	Average
P-, S-wave and resistivity	$0.30 \pm 0.26$	$0.36 \pm 0.24$	Average

<sup>1</sup> Estimate of gas hydrate concentration averaged from depth range 897–1,109 meters including zero gas hydrate concentration values.

<sup>2</sup> Estimate of gas hydrate concentration averaged from depth range 897–1,109 meters excluding zero gas hydrate concentration values.

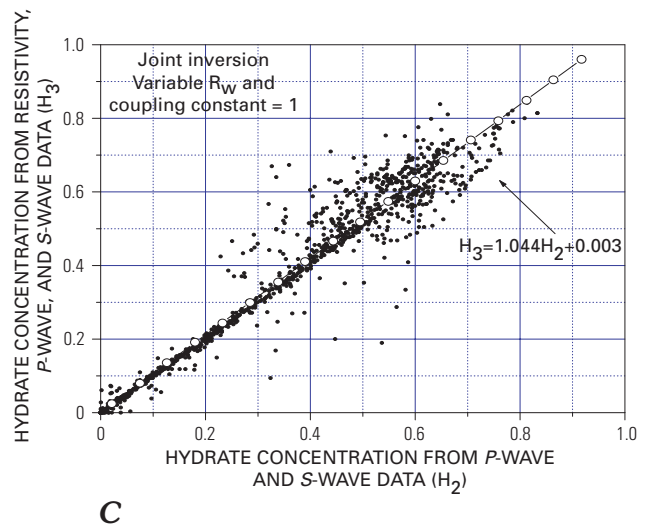
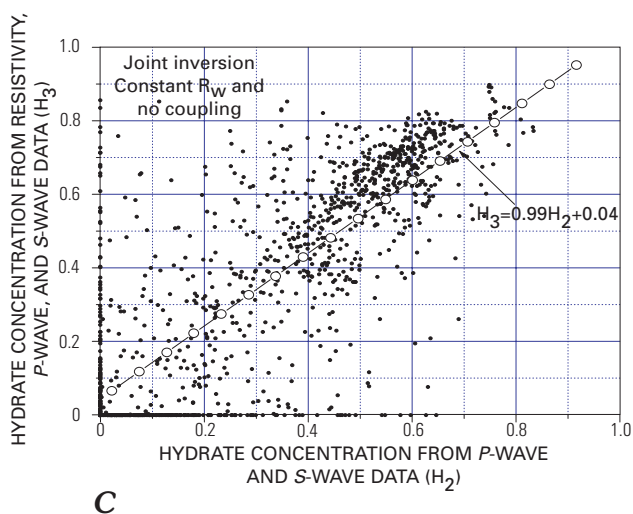
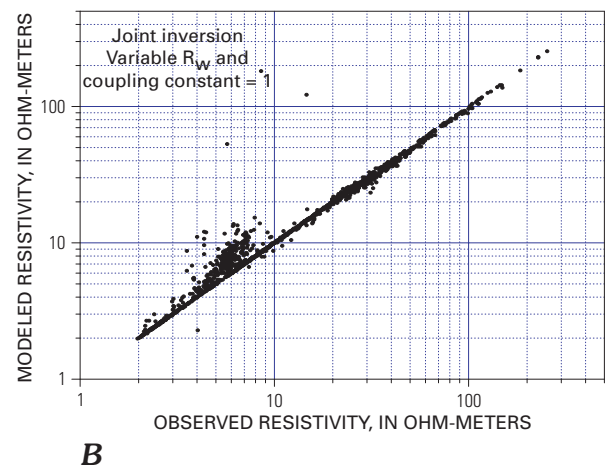
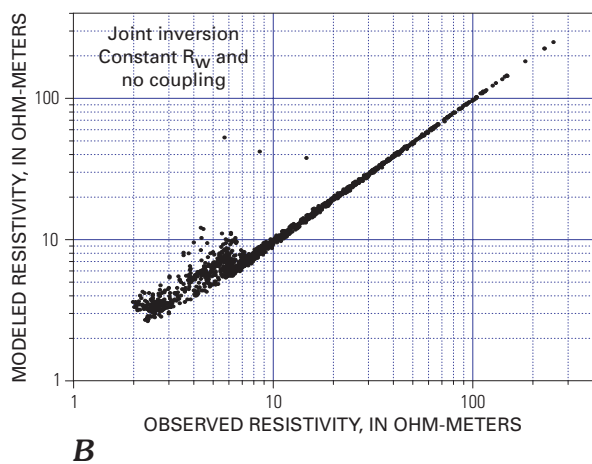
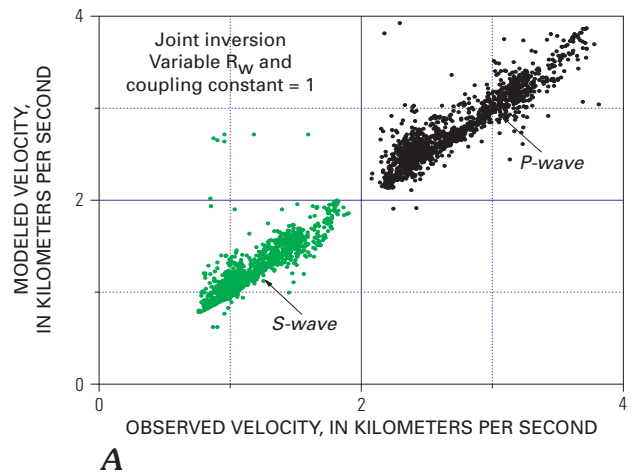
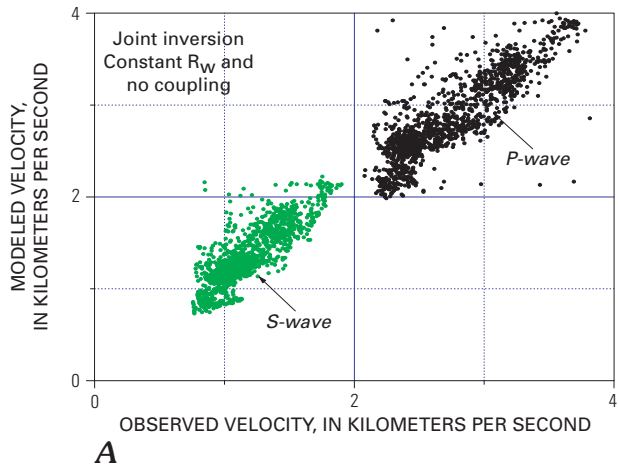


**Figure 3.** Graph showing the result of joint inversion of acoustics and resistivity. Only gas hydrate concentration ( $c$ ) with a constant resistivity of connate water  $R_w = 0.4$  ohm-meter (ohm-m) was estimated. **A**, Cross plot of modeled velocities versus observed velocities. **B**, Cross plot of modeled resistivity versus observed resistivity. **C**, Cross plot of gas hydrate concentration estimated from acoustics versus that estimated from the joint inversion of acoustics and resistivity.

**Figure 4.** Graph showing the result of the modified joint inversion of acoustics and resistivity with a coupling constant  $\gamma = 1$ . Both gas hydrate concentration ( $c$ ) and the resistivity of connate water ( $R_w$ ) were simultaneously estimated. **A**, Cross plot of modeled velocities versus observed velocities. **B**, Cross plot of modeled resistivity versus observed resistivity. **C**, Cross plot of gas hydrate concentration estimated from acoustics versus that estimated from the joint inversion of acoustics and resistivity.

The accuracy of the predicted velocity from MJI is between those of OJI with variable  $R_w$  and OJI with a constant  $R_w$ .

Figure 4B shows the modeled and observed resistivity (from PSR inversion). Like the results for the velocities, the accuracy of predicted resistivity is between that from Model 1 (OJI with a variable  $R_w$ ) and that from Model 2 (OJI with a constant  $R_w$ ).

A comparison of estimated gas hydrate concentration using only acoustic data (PS inversion) and acoustic and resistivity data (PSR inversion) is shown in figure 4C. A least-squares fitting curve indicates that the gas hydrate concentration from PSR inversion is about 4 percent higher than that from the PS inversion.

Figure 5 shows the estimated  $R_w$  for figure 4's example, and the observed resistivity ( $R_t$ ) with respect to depth. The general trend of the estimated  $R_w$  with respect to the depth is similar to the result of OJI, but the estimated  $R_w$  is somewhat less than that from OJI. A least-squares fitting curve for the estimated  $R_w$  is given by  $R_w = 1.2 - 0.00071D$ , where  $D$  is depth in meters. At  $D = 1,000$  m, the estimated  $R_w$  is 0.49 ohm-m.

Table 2 and figure 4 show that the result of MJI is between the results from Model 1 and Model 2, which indicates that the resistivity measurement contributed to the estimation of gas hydrate concentration using MJI with  $\gamma=1$  when  $c$  and  $R_w$  are simultaneously estimated. The degree of contribution of the resistivity to the inversion result is somewhat controlled by the magnitude of the coupling constant ( $\gamma$ ), which will be addressed later.

In summary, the preceding results imply that the joint inversion estimating  $c$  and  $R_w$  simultaneously is feasible. The result of OJI estimating  $c$  and  $R_w$  simultaneously from acoustic and resistivity data demonstrates that OJI is closely similar to a

sequential estimation of gas hydrate concentration based on using acoustic and  $R_w$  from resistivity data using the estimated gas hydrate concentration as input. However, the results of MJI indicate the possibility of a way to control the contribution of acoustic and resistivity measurement to the inversion, even though the coupling between the acoustic and resistivity is arbitrary.

## Discussion

### Weighted Error

The solution of the modified joint inversion using arbitrary non-zero constants for the  $G_{12}$  and  $G_{22}$  can be written as

$$c^{n+1} = c^n + Q_{11}E_1 + Q_{12}E_2 + Q_{13}E_3$$

$$R_w^{n+1} = R_w^n + Q_{21}E_1 + Q_{22}E_2 + Q_{23}E_3 \quad (13)$$

where  $Q_{ij}$  represents the element of the generalized inverse of  $G_w$ . Based on the data set from the Mallik 2L-38 gas hydrate research well, the average slowness of the observed  $P$ -wave is  $0.375 \pm 0.052$  seconds per kilometer (s/km), the average slowness of  $S$ -wave is  $0.894 \pm 0.184$  s/km, and the average resistivity is  $18.60 \pm 26.43$  ohm-m. Let  $\Delta S_p/S_p$ ,  $\Delta S_s/S_s$ , and  $\Delta R_t/R_t$  be fractional errors in  $P$ -wave slowness,  $S$ -wave slowness, and resistivity respectively. If the fractional errors are of the same magnitude or similar, then  $\Delta R_t \gg \Delta S_s > \Delta S_p$ , because the magnitude of the resistivity is much higher than the magnitude of the slowness and  $S$ -wave slowness is higher than the  $P$ -wave

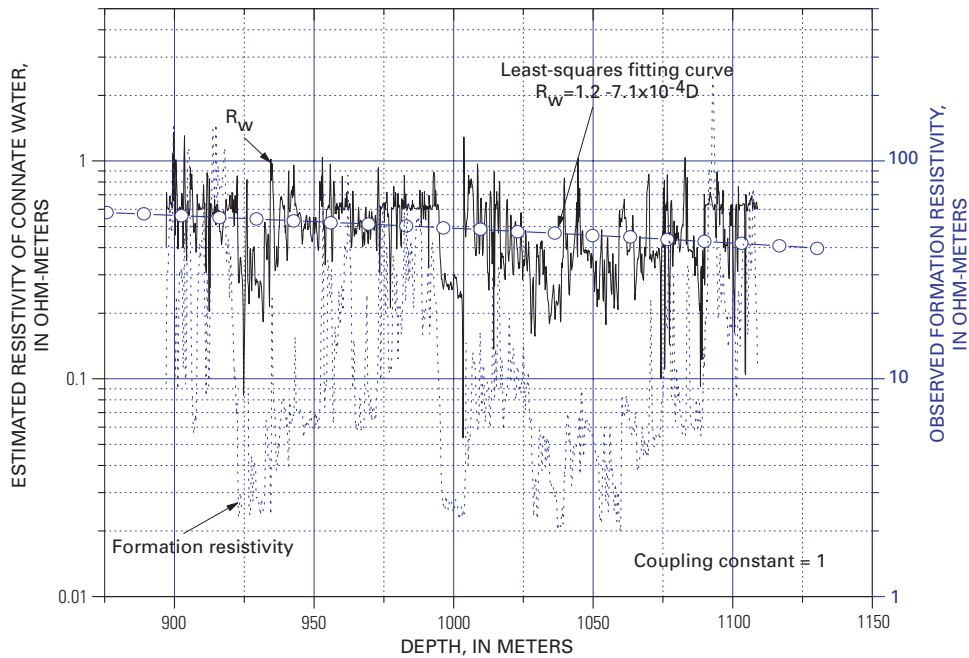


**Figure 5.** Graph showing estimated resistivity of connate water ( $R_w$ ) using modified joint inversion with a coupling constant  $\gamma=1$  and observed formation resistivity with respect to depth.  $D$ , depth in meters.

slowness. If a least-squares error is not weighted, the solutions shown in Equation (13) are affected mostly by  $E_3$ , which is  $\Delta R_t$ . So the solution can be approximated by

$$\begin{aligned} c^{n+1} &\approx c^n + Q_{13} \Delta R_t \\ R_w^{n+1} &\approx R_w^n + Q_{23} \Delta R_t \end{aligned} \quad (14)$$

Therefore, when an unweighted error is used for the joint inversion, Equation (14) implies that  $P$ -wave and  $S$ -wave do not contribute much to the joint inversion, and the estimation of hydrate concentration is dominated by the resistivity measurement. At the same time, Equation (14) indicates that  $R_w$  and  $c$  are not well constrained, because the error in  $R_t$  controls both the  $c$  and  $R_w$  simultaneously.

When the weighted error is used, the magnitudes of  $E_i$ 's are on the same order of magnitude. Therefore, each measurement contributes to the estimation of gas hydrate concentration and resistivity of connate water.

## Simultaneous Estimation of $c$ and $R_w$

Estimating  $c$  and  $R_w$  by simultaneously using the joint inversion method is problematic as mentioned previously, mainly because only the resistivity, and not the acoustics, depends on both  $c$  and  $R_w$ . In consequence, some of the elements of the Jacobian matrix are zero. This leads to the decoupling of the resistivity from the estimation of gas hydrate concentration as shown in Equation (11). In order to overcome this problem, a modified joint inversion formula was introduced. However, because the coupling constant ( $\gamma$ ) is not based on a physical principle and  $c$  depends on  $R_w$ , the result of  $R_w$  estimation should be checked against other estimates.

Miyairi and others (1999) estimated the  $R_{wa}$ , which is defined by  $R_{wa} = R_t \phi^m / a$ , from the resistivity logs. The  $R_{wa}$  should be equal to the  $R_w$  in clean water-bearing formations. According to Miyairi and others (1999), the resistivity of connate water for the non-gas-hydrate-bearing sediment at the Mallik 2L-38 varies between 0.2 and 0.5 ohm-m and decreases as depth increases. As shown in figure 2, the majority of estimated  $R_w$  from OJI varies between 0.2 and 1.0 ohm-m and decreases with depth. Miyairi and others (1999) used  $R_w = 0.48, 0.38, \text{ and } 0.29$  ohm-m for the depth intervals of 814–933 m, 933–1,076 m, and 1,076–1,150 m, respectively. The estimated  $R_w$  from OJI is 0.85, 0.57, and 0.34 ohm-m for the average depth interval of 873 m, 1,004 m, and 1,113 m respectively. Comparing the result of OJI inversion and Miyairi and others (1999), the rate of resistivity decrease with depth is similar, but  $R_w$  values differ by 0.05–0.4 ohm-m. The result from MJI indicates that the estimated  $R_w$  values vary slightly from the OJI values, being 0.58, 0.49, and 0.41 ohm-m for the depths of 873 m, 1,004 m, and 1,113 m respectively, which are about 30 percent higher than those used by Miyairi and others (1999).

## Behavior of the Joint Inversion Method

Inversion results indicate that the coupling constant ( $\gamma$ ) in the Jacobian matrix controls the amount of coupling between the

acoustics and resistivity in the estimation of gas hydrate concentration. When  $\gamma=0$ , the modified joint inversion reverts to the original joint inversion method, and the gas hydrate estimation is controlled mostly by the acoustical properties, receiving minimal contributions from the resistivity measurements, as indicated in figure 1.

The result of modified joint inversion using  $\gamma=5$ , shown in figure 6, is almost identical to that from the  $R$  inversion (table 3). Numerical tests indicate that as  $\gamma$  increases, the estimated gas hydrate concentration from a joint inversion of acoustic and resistivity approaches the result of inversion using only resistivity, and the estimated  $R_w$  approaches a constant value, which is the initial value.

Conversely, as  $\gamma$  decreases, the result of MJI approaches that of OJI. These observations indicate that the coupling constant controls the degree of resistivity contribution to the estimation of gas hydrate concentration using the joint inversion. However, it is difficult to predict the general behavior of inversion results with respect to the coupling constant, except for low and high constant values.

## Understanding the Coupling Constant

The modified joint inversion formula can be better understood if we assume that erroneous  $P$ -wave and  $S$ -wave values are used in the following way when computing the Jacobian matrix:

$$\begin{aligned} S_p^e &= S_p^t + \gamma R_w \\ S_s^e &= S_s^t + \gamma R_w \end{aligned} \quad (15)$$

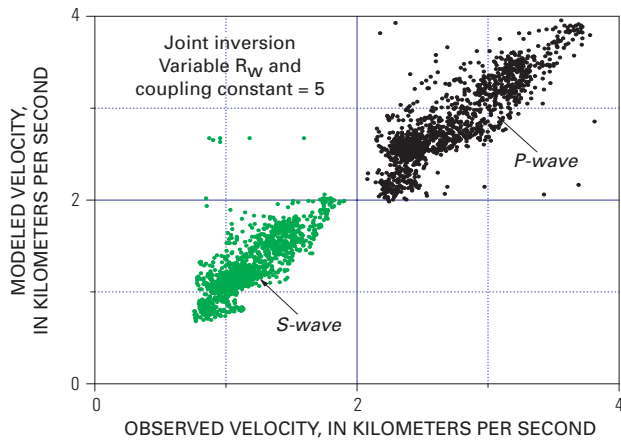
where the superscript  $t$  indicates the true computed values from the theory and the superscript  $e$  indicates the altered values used in the inversion. Then,  $G_{12} = \gamma$  and  $G_{22} = \gamma$ . Note that only elements of the Jacobian matrix, not the theoretical values, are altered.

If  $\gamma$  becomes small, the erroneous theoretical values used in the modified joint inversion approach the true values. In this case, the solution of the modified inversion approaches the solution of the original inversion shown in Equation (11).

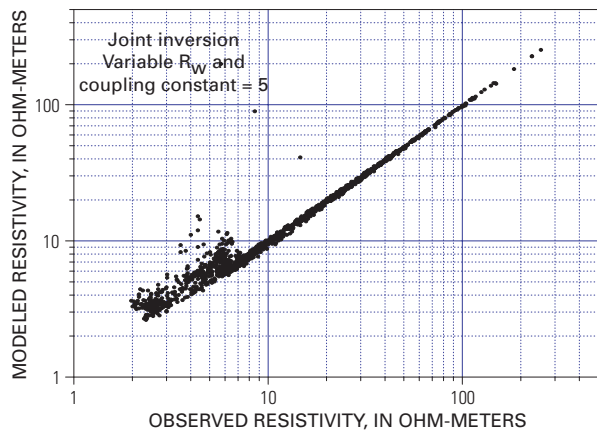
If  $\gamma$  is large, the acoustic model fails to fit the observation accurately and errors become large. When the error of computed slowness is large, Equation (1) indicates that the relative contribution of  $G_{11}$  and  $G_{21}$  compared to  $G_{12}$  and  $G_{22}$  to the overall inversion is insignificant. Therefore,  $G_{11} \approx 0$  and  $G_{21} \approx 0$  as  $\gamma$  becomes large. In this case, the solution can be written as

$$\begin{aligned} c^{n+1} &\approx c^n + \frac{2\gamma^2 G_{31} E_3 - \gamma G_{31} G_{32} (E_1 + E_2)}{2\gamma^2 G_{31}^2} \\ &\approx c^n + \frac{E_3}{G_{31}} \text{ as } \gamma \rightarrow \infty \text{ and} \\ R_w^{n+1} &\approx R_w^n + \frac{E_1 + E_2}{2\gamma} \approx R_w^n \text{ as } \gamma \rightarrow \infty \end{aligned} \quad (16)$$

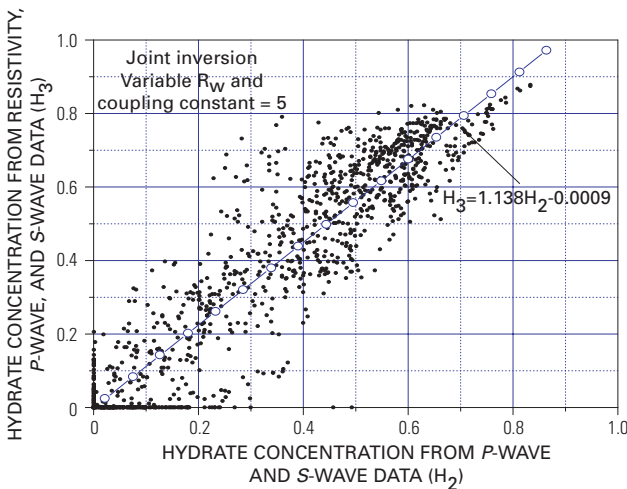
Equation (16) indicates that as the coupling constant becomes larger,  $E_3$  or the resistivity measurement dominates the estimation of  $c$ , and the change of  $R_w$  is insignificant or  $R_w$  approaches the initial value.



**A**



**B**



**C**

**Figure 6.** Graph showing the result of the modified joint inversion of acoustics and resistivity with a coupling constant  $\gamma=5$ . Both gas hydrate concentration ( $c$ ) and the resistivity of connate water ( $R_w$ ) were simultaneously estimated. *A*, Cross plot of modeled velocities versus observed velocities. *B*, Cross plot of modeled resistivity versus observed resistivity. *C*, Cross plot of gas hydrate concentration estimated from acoustics versus that estimated from the joint inversion of acoustics and resistivity.

Note that the solution of MJJ with a large  $\gamma$  approaches the result of OJI with a constant  $R_w$ . Equation (11) indicates that when there is no update of  $R_w$  in the inversion, the following relation should be valid:

$$G_{31}(G_{11}E_1 + G_{21}E_2) = (G_{11}^2 + G_{21}^2) E_3 \quad (17)$$

Substituting Equation (17) into Equation (11) for  $c$ , the result is

$$c^{n+1} = c^n + \frac{E_3}{G_{31}} \quad (18)$$

This is identical to the inversion solution of the resistivity and identical to Equation (16).

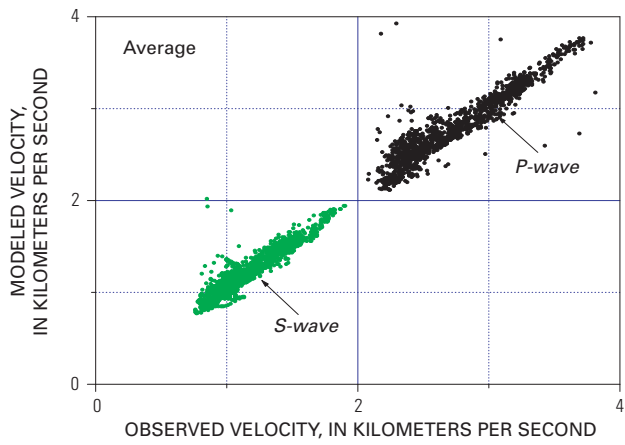
## Comparison of Various Inversion Results

Each measurement— $P$ -wave,  $S$ -wave, and resistivity—can be used separately in the inversion to estimate gas hydrate concentrations. When only  $R_t$  is used in the inversion,  $R_w$  should be an input, because of the presence of two unknowns with one observation. Table 3 shows results of the estimation of gas hydrate at the Mallik 2L-38 well from various combinations of measurements. Among all the estimates, those using only resistivity measurements yield the highest average hydrate concentrations.

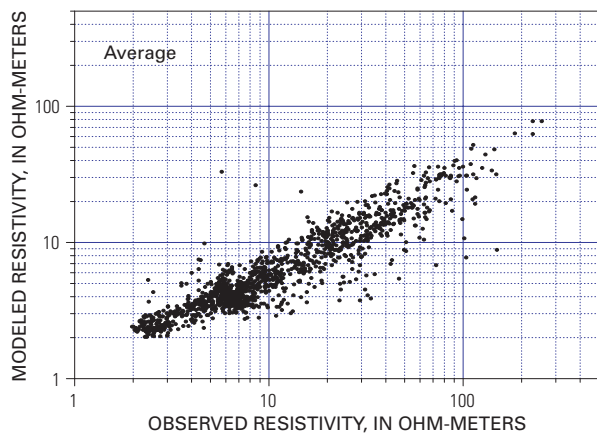
The average hydrate concentrations estimated from  $P$ -wave and  $S$ -wave slownesses are similar, but the estimated amount is less than that from resistivity by about 5 percent when all zero concentration values are included and by about 12 percent when zero concentration values are excluded. The average gas hydrate concentration estimated from the PS inversion is smaller than that from the PSR inversion with a constant  $R_w$ , or a variable  $R_w$  using MJJ with  $\gamma=1$ , but the estimates are similar to those of PSR inversion with a variable  $R_w$  using OJI.

The results of the simultaneous estimations of  $c$  and  $R_w$  from MJJ with  $\gamma=1$  indicate that the estimates of gas hydrate concentration are slightly higher, on the order of 2 percent, than that from estimates based on acoustics. Estimated gas hydrate concentrations indicate that MJJ with  $\gamma=1$  still favors acoustics, but the contribution of resistivity to the estimates is apparent, and the amount may be controlled by the value of  $\gamma$ . However, it is difficult to predict the behavior of the inversion result with respect to the coupling constant.

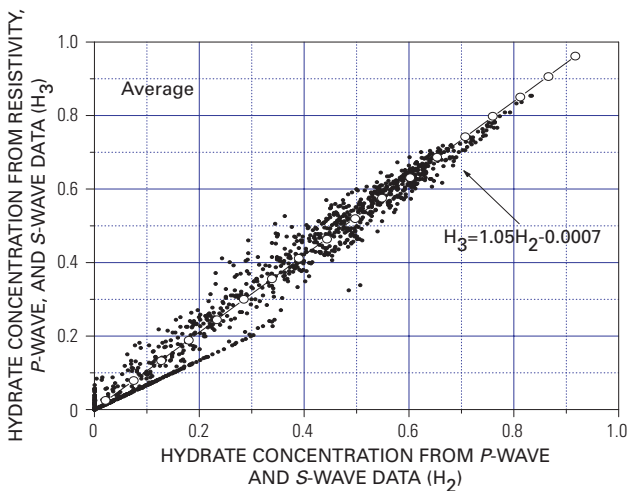
Gas hydrate concentrations by averaging each individual estimation are also shown in table 3. The gas hydrate concentrations estimated from the average of  $P$ - and  $S$ - wave estimates are similar to that of the PS inversion. Estimates based on the PSR inversion using MJJ with  $\gamma=1$  are similar to the averages of three individual estimates. But the cross plots for the modeled and observed quantities are substantially different. Figure 7 shows the result of averaging gas hydrate concentrations from separate estimations from  $P$ -wave,  $S$ -wave, and resistivity data. The modeled velocities are similar to those from MJJ with  $\gamma=1$ ; in fact, average velocities of modeled  $P$ - and  $S$ -waves are  $2.78 \pm 0.38$  km/s and  $1.23 \pm 0.26$  km/s, respectively. The only difference in the velocity estimates is the amount of scattering of the modeled velocities. However, the modeled resistivity differs markedly from the observed value (fig. 7B), being about 50 percent lower.



**A**



**B**



**C**

**Figure 7.** Graph showing the result of averaging the individual gas hydrate estimates from *P*-wave, *S*-wave, and resistivity data. *A*, Cross plot of modeled velocities versus observed velocities. *B*, Cross plot of modeled resistivity versus observed resistivity. *C*, Cross plot of gas hydrate concentration estimated from acoustics versus that estimated from the joint inversion of acoustics and resistivity.

Various inversion methods provide different estimations of gas hydrate concentrations. Judging which estimate is the most accurate one is difficult, because gas hydrate concentrations in sediments at the Mallik 2L-38 well were not accurately measured. The difference of gas hydrate estimation between resistivity and acoustics may be real, because the lateral resolution (or depth of investigation) of each logging tool is different, or the difference may be an artifact owing to the inaccuracy of acoustic models based on the weighted equation or erroneous parameters of the Archie's constants.

## Conclusion

The following conclusions can be drawn from a joint inversion of acoustics and resistivity measurements for gas-hydrate-bearing sediments.

1. Simultaneously estimating the gas hydrate concentration and the resistivity of connate water ( $R_w$ ) is problematic, because the original inversion equation for the estimation of gas hydrate concentration uses only acoustics decoupled from the resistivity measurement.

2. A modified joint inversion method, implemented by inserting a coupling constant where the element of Jacobian matrix is zero, partly compensates the adverse effect of decoupling. However, because the coupling constant is not based on the physical principles, predicting the effect of the coupling constant is difficult except at the large values.

3. The contribution of resistivity to gas hydrate estimates can be controlled in part by the magnitude of the coupling constant. As the value of the coupling constant ( $\gamma$ ) increases, the modified joint inversion favors the resistivity measurement; when  $\gamma$  decreases, MJI favors acoustics.

4. Even though  $R_w$  is constrained by *P*- and *S*-wave data through  $c$ , the estimated  $R_w$  from the modified joint inversion should be checked against  $R_w$  values estimated by other methods, because  $R_w$  is not constrained physically by acoustics.

5. When a constant  $R_w$  is used in the gas hydrate estimation, the joint inversion method has no clear advantage over the individual inversion. However, when  $c$  and  $R_w$  are estimated simultaneously, the modified joint inversion method may be preferred.

## References Cited

- Aki, Keiiti, and Richards, P.G., 1980, Quantitative seismology-theory and methods, Volume 2: San Francisco, W.H. Freeman, 932 p.
- Archie, G.E., 1942, The electrical resistivity log as an aid in determining some reservoir characteristics: *Journal of Petroleum Technology*, v. 1, p. 55–62.
- Collett, T.S., 1983, Detection and evaluation of natural gas hydrates from well logs, Prudhoe Bay, Alaska; *Proceedings of the Fourth International Conferences on Permafrost*, Fairbanks, Alaska: Washington D.C., National Academy of Sciences, p. 169–174.
- Collett, T.S., 1995, Natural gas hydrates of the Prudhoe Bay and Kuparuk River area, North Slope, Alaska: *American Association of Petroleum Geologists Bulletin*, v. 77, no. 5, p. 793–812.

- Collett, T.S., and Ladd, John, 2000, Detection of gas hydrate with down-hole logs and assessment of gas hydrate concentration (saturation) and gas volumes on the Blake Ridge with electrical resistivity log data, *in* Paul, C.K., and others, eds., *Proceedings of Ocean Drilling Program, Scientific Results: College Station, Tex.*, v. 164, p. 179–191.
- Dallimore, S.R., Collett, T.S., and Uchida, Takashi, 1999, Overview of science program, JAPEX/JNOC/GSC Mallik 2L-38 gas hydrate research well, *in* Dallimore, S.R., and others, eds., *Scientific result from JPEX/JNOC/GSC Mallik 2L-38 gas hydrate research well, Mackenzie Delta, northwest Territories, Canada: Geological Survey of Canada Bulletin 544*, p. 11–17.
- Guerin, Gilles, Goldberg, David, and Meltser, Aleksandr, 1999, Characterization of in situ elastic properties of gas hydrate-bearing sediments on the Blake Ridge: *Journal of Geophysical Research*, v. 104, p. 11781–11795.
- Lee, M.W., 1990, Traveltime inversion using transmitted waves of offset VSP data: *Geophysics*, v. 55, p. 1089–1097.
- Lee, M.W., 2000, Gas hydrate amount estimated from acoustic logs at the Blake Ridge, Sites 994, 995, and 997, *in* Paul, C.K., and others, eds., *Proceedings of Ocean Drilling Program, Scientific Results: College Station, Tex.*, v. 164, p. 193–198.
- Lee, M.W., and Collett, T.S., 1999, Amount of gas hydrate estimated from compressional- and shear-wave velocities at the JAPEX/JNOC/GSC Mallik 2L-38 gas hydrate research well, *in* Dallimore, S.R., and others, eds., *Scientific result from JPEX/JNOC/GSC Mallik 2L-38 gas hydrate research well, Mackenzie Delta, northwest Territories, Canada: Geological Survey of Canada Bulletin 544*, p. 313–322.
- Lee, M.W., Hutchinson, D.R., Collett, T.S., and Dillon, W.P., 1996, Seismic velocities for hydrate-bearing sediments using weighted equation: *Journal of Geophysical Research*, v. 101, p. 20347–20358.
- Lines, L.R., and Treitel, S., 1984, Tutorial, A review of least squares inversion and its application to geophysical problems: *Geophysical Prospecting*, v. 32, p. 159–186.
- Mathews, M.A., 1986, Logging characteristics of methane hydrate: *The Log Analyst*, v. 27, p. 26–63.
- Miyairi, M., Akihisa, K., Uchida, T., Collett, T.S., and Dallimore, S.R., 1999, Well-log interpretation of gas-hydrate-bearing formations in the JAPEX/JNOC/GSC Mallik 2L-38 gas hydrate research well, *in* Dallimore S.R., and others, eds., *Scientific result from JPEX/JNOC/GSC Mallik 2L-38 gas hydrate research well, Mackenzie Delta, northwest Territories, Canada: Geological Survey of Canada Bulletin 544*, p. 281–293.
- Sloan, E.D., Brewer, P.G., Paul, C.K., Collett, T.S., Dillon, W.P., Holbrook, W.S., and Kvenvolden, K.A., 1999, Future of gas hydrate research: *Eos*, v. 80, p. 247.
- Tarantola, A.T., 1987, *Inverse problem theory*: Amsterdam, Elsevier, 613 p.